

Disentangling residence time and temperature sensitivity of microbial decomposition in a global soil carbon model

J.-F. Exbrayat^{1,*}, A. J. Pitman¹ and G. Abramowitz¹

[1]{ARC Centre of Excellence for Climate System Science and Climate Change Research Centre, University of New South Wales, Sydney, New South Wales, Australia}

*Now at: School of GeoSciences and National Centre for Earth Observation, University of Edinburgh, Edinburgh, UK

Correspondence to: J.-F. Exbrayat (j.exbrayat@ed.ac.uk)

Abstract

Recent studies have identified the first-order representation of microbial decomposition as a major source of uncertainty in simulations and projections of the terrestrial carbon balance. Here, we use a reduced complexity model representative of current state-of-the-art models of soil organic carbon decomposition. We undertake a systematic sensitivity analysis to disentangle the effect of the time-invariant baseline residence time (k) and the sensitivity of microbial decomposition to temperature (Q_{10}) on soil carbon dynamics at regional and global scales. Our simulations produce a range in total soil carbon at equilibrium of ~592 to 2745 Pg C which is similar to the ~561 to 2938 Pg C range in pre-industrial soil carbon in models used in the fifth phase of the Coupled Model Intercomparison Project. This range depends primarily on the value of k , although the impact of Q_{10} is not trivial at regional scales. As climate changes through the historical period, and into the future, k is primarily responsible for the magnitude of the response in soil carbon, whereas Q_{10} determines whether the soil remains a sink, or becomes a source in the future mostly by its effect on mid-latitudes carbon balance. If we restrict our simulations to those simulating total soil carbon stocks consistent with observations of current stocks, the projected range in total soil carbon change is reduced by 42% for the historical simulations and 45% for the future projections. However, while this observation-based selection dismisses outliers it does not increase confidence in the future

30 sign of the soil carbon feedback. We conclude that despite this result, future estimates of soil
31 carbon, and how soil carbon responds to climate change should be constrained by available
32 observational data sets.

33

34 **1 Introduction**

35 There is a 6-fold range in the amount of carbon stored in the soil in simulations conducted as
36 part of the fifth phase of the Coupled Model Intercomparison Project (CMIP5; Taylor et al.,
37 2012). This 6-fold range, identified by Todd-Brown et al. (2013), is consistent with results
38 from the recent model intercomparison projects such as the Coupled Climate-Carbon Cycle
39 Model Intercomparison Project (C⁴MIP; Friedlingstein et al., 2006). The analysis of carbon
40 stores in both C⁴MIP and CMIP5 have focused on the prediction of terrestrial and soil carbon
41 through time. In addition to demonstrating the large differences in carbon stocks (Todd-
42 Brown et al., 2013), they have also highlighted large inter-model differences in global and
43 regional land-atmosphere carbon (C) fluxes (e.g. Friedlingstein et al., 2006, 2014). This lack
44 of agreement between simulations exists in fully coupled models (e.g. C⁴MIP and CMIP-5)
45 but can also be found if sources of uncertainty are narrowed by relying on one weather
46 dataset to drive multiple land models (Friend et al., 2013; Nishina et al., 2014), or by using
47 one land model driven by multiple climate projections (Ahlström et al., 2013).

48 In these previous studies, critical uncertainties have been identified in the microbial
49 decomposition of soil organic C and the associated release of CO₂ via heterotrophic
50 respiration (R_h). This is despite all the current state-of-the-art global soil C models relying on
51 a similar representation of decomposition as a first-order process (see Exbrayat et al., 2013b;
52 Nishina et al., 2014; Todd-Brown et al., 2013). This conceptualization describes
53 decomposition and R_h as proportional to the availability of organic matter. The decay rate (or
54 R_h per unit of soil C) is modified based on an environmental scalar that intends to mimic the
55 dynamical response of microbial biomass to soil moisture and soil temperature.

56 This simple model structure has recently received some criticism because of its lack of
57 explicit representation of microbial physiology (Allison et al., 2010; Todd-Brown et al.,
58 2012; Wieder et al., 2013; Xenakis and Williams, 2014). However, it can successfully explain
59 some complex dynamic processes including the acclimation of decomposers to warming (Luo

60 et al., 2001) as a result of the quick depletion of labile pools by enhanced microbial biomass
61 (Kirschbaum, 2004; Knorr et al., 2005).

62 We previously identified (Exbrayat et al., 2013b, 2014) some further implications of the first-
63 order representation of microbial decomposition. First, in climate change experiments, model
64 pools are usually initialised using a spin-up procedure with fixed pre-industrial atmospheric
65 CO₂ concentrations until C pool trends are removed (Xia et al., 2012). Due to the interaction
66 with substrate availability, the decay rate simulated by the model in response to steady
67 boundary conditions determines the size of soil C pools reached at equilibrium. Because spin-
68 up is a long computational process, the magnitude of pool sizes is conserved during
69 subsequent shorter simulations of climate change and, as a result, equilibrated stocks strongly
70 explain final stocks (e.g. CMIP5 models as shown in supplementary Figure S1 after Exbrayat
71 et al., 2014). Second, the microbial sensitivity to changing environmental conditions affects
72 the response of the system under transient climate simulations (Falloon et al., 2011; Exbrayat
73 et al., 2013a,b). However, because substrate availability also controls the amount of respired
74 carbon, there is a “memory” control imposed by the initial conditions of this transient
75 simulation (Exbrayat et al., 2013b and 2014) that also affects the response to perturbation in
76 boundary conditions. The relative contribution of these two factors on soil C projections
77 remains to be explored in detail especially since last generation models disagree on the
78 carbon balance projected in the future (Friedlingstein et al., 2014; Nishina et al., 2014),
79 making it challenging to elaborate any land-based offsetting strategy.

80 Here, we use a reduced complexity model representative of current state-of-the-art models of
81 soil organic C decomposition. A systematic sensitivity analysis is performed to disentangle
82 the effect of the time-invariant baseline residence time and the formulation of the dynamic
83 response of microbial decomposition to climatic change on soil C dynamics at regional and
84 global scale.

85

86 **2 Materials and methods**

87 **2.1 Reduced complexity model**

88 It is not possible to re-run each CMIP5 model or isolate the representation of soil carbon
89 processes from each model. We therefore use a reduced complexity model that simulates the

90 monthly evolution of a single soil organic carbon pool, C_s , in response to input derived from
 91 Net Primary Productivity (NPP , $\text{g C m}^{-2} \text{ mth}^{-1}$) and output by heterotrophic respiration (R_h , g
 92 $\text{C m}^{-2} \text{ mth}^{-1}$). For each monthly time step, the soil carbon balance can be described as:

$$93 \quad \frac{\partial C_s}{\partial t} = NPP - R_h \quad (1)$$

94 where NPP is a prescribed boundary condition in our model and R_h is simulated as a first-
 95 order process dependent on the availability of substrate C_s such as:

$$96 \quad R_h = k^{-1} \times f_T \times f_W \times C_s \quad (2)$$

97 where k is the baseline residence time at 15°C (Xia et al., 2013) adjusted at each time step by
 98 f_T which is a function of soil temperature T_s ($^\circ\text{C}$). The soil moisture (θ_s) modification
 99 function, f_W , is usually expressed as a fraction of soil moisture saturation (Moyano et al.,
 100 2012). We implement a classical formulation of the soil temperature sensitivity function f_T :

$$101 \quad f_T = Q_{10}^{\frac{(T_s - T_{ref})}{10}} \quad (3)$$

102 where Q_{10} is a constant factor that describes the relative increase in microbial activity for a
 103 warming of 10°C , and T_{ref} is the reference temperature ($^\circ\text{C}$) for which $f_T(T_s) = 1$ (Lloyd and
 104 Taylor, 1994; Bauer et al., 2012). The chosen T_{ref} is the commonly used 15°C (Todd-Brown
 105 et al., 2013) so that the decomposition rate equals k^{-1} when moisture is non-limiting and
 106 temperature is approximately equal to the global average. We use the same formulation of f_W
 107 as in the CASA-CNP model (Wang et al., 2010):

$$108 \quad f_W(\theta_s) = \left(\frac{\theta_s - 1.70}{0.55 - 1.70} \right)^{6.6481} \times \left(\frac{\theta_s + 0.007}{0.55 + 0.007} \right)^{3.22} \quad (4)$$

109 which is a bell-shaped function that is equal to 1 for $\theta_s = 0.55$.

110 This first-order representation of microbial decomposition with a specified decay rate
 111 adjusted by environmental scalars is used in all 11 CMIP5 models that simulate soil carbon
 112 (Todd-Brown et al., 2013) and all 7 Dynamic Global Vegetation Models used in the ISI-MIP
 113 project (Friend et al., 2013; Nishina et al., 2014). Typically, these models rely on a multi-pool
 114 architecture to represent the diversity in organic matter. Each pool has its own residence time
 115 that corresponds to a degree of resistance to decomposition (Davidson and Janssen, 2006).
 116 Usually, part of the decomposition occurring in one pool is routed to one or several other

117 pools while the rest is emitted via R_h . At the ecosystem scale, however, the same
118 environmental scalar is applied despite the multi-pool architecture, and the heterotrophic
119 respiration flux is proportional to the amount of substrate available. Therefore, our simplified
120 model is broadly representative of the current paradigm and provides a useful framework to
121 undertake the sensitivity analysis described hereafter.

122 Soil moisture also has an influence on microbial decomposition (Falloon et al., 2011, Moyano
123 et al., 2012, 2013; Exbrayat et al., 2013a,b). However, Todd-Brown et al. (2013) recently
124 demonstrated that a one pool reduced complexity model could reproduce both total soil
125 carbon content and its spatial distribution for most of the CMIP5 models without considering
126 decomposition response to variations in soil moisture. We also recently showed that global
127 features in the distribution and evolution of C_s were much more related to uncertainties in f_T
128 than uncertainties in the formulation of f_W (Exbrayat et al., 2013b). Therefore, in order to
129 keep the analyses as simple as possible and isolate the effect of f_T but still account for the
130 effect of soil moisture on R_h , we keep the formulation of f_W constant in the experiments that
131 follow.

132 We are aware of that our reduced complexity model relies on questionable assumptions such
133 as the use of a single soil carbon pool and global values of k , Q_{10} and T_{ref} . However, while we
134 agree that a multiple pool structure would provide diverging results, single pool soil carbon
135 carbon models similar to our design are used in 3 of the 11 CMIP5 models described by
136 Todd-Brown et al. (2013) and 2 of the 7 ISI-MIP models described by Nishina et al. (2014).
137 Further, using global parameter values of k , Q_{10} and T_{ref} is consistent with these state-of-the-
138 art models (Todd-Brown et al., 2013; Nishina et al., 2014). Of course, this does not allow
139 representing processes such as the remobilization of carbon in the active cycle following
140 permafrost thaw (Koven et al., 2011) or the probably different behaviour of biological
141 systems in frozen conditions but these are not routinely implemented in the land component
142 of Earth system models and therefore fall beyond the scope of this paper. In summary, we
143 wish to reiterate that this study investigates the sensitivity of the first-order parameterization
144 of microbial decomposition and R_h processes used in current ecosystem models to its
145 uncertain parameters (Todd-Brown et al., 2013; Nishina et al., 2014). We do not intend to
146 provide improved results of the response of soil carbon to climate change but rather illustrate
147 and better understand the implications of the current ubiquitous approach to parameterization
148 and initial value prescription described in Section 2.2.

149 2.2 Model setup and experiments

150 We configure the reduced complexity model in a spatially explicit way to represent global
151 variations, implemented as a surrogate for the CASA-CNP biogeochemical module (Wang et
152 al., 2010) of the CABLE land surface model (Wang et al., 2011). A previous simulation by
153 CABLE coupled to the coarse-resolution CSIRO Mk3L climate model (3.2° latitude \times 5.6°
154 longitude; Phipps et al., 2011) and driven by CMIP5 atmospheric CO_2 data provides monthly
155 NPP , T_s and θ_s to the reduced complexity model. We use both historical simulations
156 (Exbrayat et al., 2013b) and 21st century projections using the Representative Concentration
157 Pathway 8.5 (RCP 8.5) atmospheric concentration scenario.

158 We perform a sensitivity analysis by running the simple model with various combinations of
159 a Q_{10} value and a baseline residence time k . We use 11 equally-spaced values of Q_{10} ranging
160 from 1.5 to 2.5 (i.e. intervals of 0.1), and 31 equally-spaced values of k ranging from 120
161 months to 480 months (i.e. intervals of 12 months). These values are based on the range of
162 results previously obtained by Todd-Brown et al. (2013) with their own reduced complexity
163 model. Each value of Q_{10} is applied with each value of k for a total of 341 simulations. Model
164 versions are initialised via a classical spin-up procedure (Xia et al., 2012) using input data
165 from 1850 to 1859 for 10,000 years to ensure all soil carbon pools reach a steady-state. We
166 then continue simulations with NPP , T_s and θ_s data from 1850 to 2005, and continue with
167 RCP 8.5 projections to 2100. We note that these drivers do not include the representation of
168 land-use and land cover change and their effect on NPP , T_s and θ_s . Therefore, SOC input are
169 likely to be higher than in reality. However, as stated earlier we are using the reduced
170 complexity framework to understand the behaviour of the SOC model in response to
171 variations in its parameters and we do not aim to provide improved estimates of global scale
172 terrestrial carbon sinks. In each model version, both k and the sensitivity of R_h to temperature
173 (represented by Q_{10}) are constant globally, in accordance with observations (Mahecha et al.,
174 2010) and state-of-the-art models (Todd-Brown et al., 2013; Nishina et al., 2014). However,
175 the actual value of the environmental scalar f_T will of course vary spatially and temporally as
176 a function of T_s . As we keep the same formulation of f_w between model versions, we can
177 attribute differences in results to the values of Q_{10} or k .

178

179 **2.3 Harmonized World Soil Database**

180 The Harmonized World Soil Database (HWSD; FAO, 2012) combines several national
181 inventories and provides a number of chemical and physical soil properties at a 30 arc second
182 resolution globally. However, despite the availability of this dataset, CMIP5 models exhibit a
183 six-fold range in their total soil carbon content (Todd-Brown et al., 2013) including values
184 well outside the uncertainty boundaries of observational data. We showed previously that
185 using this dataset to discriminate between acceptable and unacceptable simulations resulted
186 in a non-negligible reduction of the uncertainty in historical net carbon uptake (Exbrayat et
187 al., 2013b). While we do not aim to provide CMIP5-like projections of the soil carbon
188 balance with our reduced complexity model, we investigate the value of using the HWSD to
189 discriminate between plausible and implausible simulations.

190 We follow the method described by Todd-Brown et al. (2013) to derive an estimate of current
191 total soil carbon from the latest version of the Harmonized World Soil Database (HWSD).
192 First, we re-grid the original 30 arc seconds raster to a $0.5^\circ \times 0.5^\circ$ resolution. Within each
193 half-degree cell we select the dominant soil type. For each soil type, the database provides
194 bulk density and organic carbon content for a top layer (0 – 30 cm depth) and a bottom layer
195 (30 – 100 cm depth). This allows us to calculate soil C density (in kg C m^{-2}) in each cell. We
196 then multiply each grid cell by its area and sum to obtain a global estimate of ~ 1170 Pg C.
197 Similarly to Todd-Brown et al. (2013) we also consider the uncertainty associated to our re-
198 gridding process as well as analytical measurements of soil properties. We therefore obtain a
199 95% confidence interval (CI_{95}) of 29% below the mean to 32% above the mean, or $\sim 830 -$
200 1550 Pg C. We provide these gridded data as supplementary material.

201

202 **3 Results**

203 **3.1 Total soil carbon and global balance**

204 Figure 1 presents snapshots of total soil carbon for all 341 model versions for three periods:
205 at equilibrium (in 1850, Figure 1a), at the end of historical transient simulations (in 2005,
206 Figure 1b), and at the end of the projections with forcing corresponding to RCP 8.5 (in 2100,
207 Figure 1c). Figure 1a shows that the spin-up procedure causes different model versions to
208 equilibrate at widely varying levels of total soil carbon despite the use of the same boundary

209 conditions of NPP and T_s . Differences in residence time k contribute most of the ~592 to
210 2745 Pg C range, with larger values of k resulting in larger pools (Figure 1a). Variations in
211 the Q_{10} parameter of f_T have a smaller influence on total soil carbon but lower values do result
212 in lower total soil carbon. For the same value of k , simulations with $Q_{10} = 1.5$ equilibrate with
213 total soil carbon equal to $86\% \pm 0.005\%$ (mean ± 1 standard deviation) of the amount with
214 $Q_{10} = 2.5$. Figure 1b shows that the distribution of total soil carbon between model versions
215 does not vary much during historical simulations (1850-2005). Models with large total soil
216 carbon pools over this period remain versions with long residence time k and higher values of
217 Q_{10} . Note, however, that the range of total soil carbon in 2005 grows to ~709 to 2943 Pg C.
218 Dashed contours on Figure 1b indicate the limits of the CI₉₅ of the HWSD for current total
219 soil carbon. Here, 115 simulations with values of k ranging approximately from 150 to 250
220 months all fall within this range for 2005, regardless of the Q_{10} value used. Finally, Figure 1c
221 continues to indicate a strong control of k on the total soil carbon in 2100. The projected
222 range narrows to ~684 to 2825 Pg C throughout the 21st century. However, we note there is
223 an inversion in the influence of Q_{10} on simulated total soil carbon with lower values of Q_{10}
224 resulting in larger pools especially for longer baseline residence times k . Nevertheless, this is
225 still minor compared to the influence of k on C_s .

226 Although the range in simulated soil carbon remains similar through time, non-negligible
227 changes occur. This is highlighted in Figure 2 which shows ΔC_s , the change in total soil
228 carbon as a function of model parameters k and Q_{10} for the historical simulations (1850 –
229 2005, Figure 2a) and RCP 8.5 projections (2006 – 2100, Figure 2b). First, Figure 2a clearly
230 shows that all model versions act as a net carbon sink during historical simulations,
231 accumulating between 81 and 283 Pg C. Model versions with longer residence time k tend to
232 accumulate more carbon through time. However, models with the largest value of Q_{10} tend to
233 accumulate only $69\% \pm 0.4\%$ (mean ± 1 standard deviation) of the amount that the lowest Q_{10}
234 models do. By analysing Figure 2b, we see that the influence of Q_{10} on the total soil carbon
235 balance grows during RCP 8.5 projections where Q_{10} now determines whether the soil
236 remains a sink or becomes a source. This change between a source or a sink for different Q_{10}
237 values follows a near linear relationship with k (solid line on Figure 2b). Interestingly, the -
238 179 to 168 Pg C range in the change in total soil carbon during RCP 8.5 is mostly a function
239 of Q_{10} as both extremes are achieved with the longest residence time used here. In other

240 words, while Q_{10} decides of the sign of the change, k , and hence the initial stocks of SOC
241 after spin-up, drives the magnitude of the response.

242 If we consider only models that fall within the CI_{95} of the HWSD for current total soil carbon
243 (dashed contours on Figure 2a and 2b) the spread in simulated total soil carbon balance is
244 largely reduced. During the historical simulations, the range of this subset of models shrinks
245 by 84 Pg C to between 87 and 205 Pg C. It corresponds to a reduction of about 42% of the
246 initial uncertainty. Similarly, the range in projected soil carbon balance is reduced by 157 Pg
247 C to -129 to 61 Pg C, a reduction of about 45% of the initial uncertainty. We note, however,
248 that this restriction does not necessarily increase confidence in sign of the future soil carbon
249 change under RCP8.5.

250 Differences in the behaviour between the full set of models and this subset of observationally
251 constrained models can be seen in the time series and probability density functions (PDFs)
252 for the historical period, shown in Figure 3. First, the time series from 1850 shows there is no
253 noticeable difference between the full set of simulations (in grey) and the subset of
254 simulations with acceptable current soil carbon (in green) until 1900. During the first half of
255 the 20th century, stronger sinks are excluded as they lie outside the CI_{95} range, which
256 correspond to the upper tail of the distribution of ΔC_s (see PDF inset for 1950). However, the
257 kurtosis of the distribution, or most probable change from our simulations, changes
258 negligibly. After ~1960, we observe a step-change in cumulative ΔC_s that follows a strong
259 response in NPP to the rapid increase in atmospheric CO_2 (please refer to Exbrayat et al.,
260 2013b for a more detailed account of this behaviour). The spread between simulations grows
261 and most of the excluded simulations based on the CI_{95} range are the strongest sinks (as in
262 Figure 2a) while a few of the least accumulating simulations are also excluded. This does
263 have a large impact on the most probable change in storage, reducing it from ~200 PgC to
264 ~140 PgC.

265 We now examine future simulations and present time series and PDFs of change in total soil
266 carbon during RCP 8.5 projections in Figure 4. All simulations continue to accumulate
267 carbon at the beginning of the 21st century and remain net carbon sinks until about 2060. At
268 the end of the century, some model versions have simulated positive ΔC_s corresponding to a
269 net carbon sink over the 21st century, while other ends their projections with negative ΔC_s , or
270 a net carbon loss. However, all simulations show the same overall behaviour with first an
271 increase in C_s that peaks, and then a decrease in C_s . The timing of the peak, i.e. when soil

272 carbon starts to deplete, varies between ~2035 and 2075 and is explained by the value of Q_{10}
273 ($R^2 = 0.74$, data not shown) with higher values leading to an earlier peak. This indicates that,
274 in all simulations, soil has become a net source of carbon by the end of the 21st century,
275 regardless how much carbon was accumulated since 2005, and hence since 1850. The PDFs
276 in 2050 show that selecting only observationally consistent models results in the most heavily
277 accumulating simulations, i.e. those that would peak later, to be dismissed. However, by
278 2100, both the lower and upper tails of the initial distribution are clipped, reducing the
279 simulated range from -178 to 168 Pg C (all simulations) to -129 to 61 Pg C. In both cases,
280 differences in the kurtosis of both distributions remains very small which indicates that our
281 selection scheme dismisses outliers. We note that the lower bound of ΔC_s for both sets of
282 models is the same until late in the projections (~2085).

283

284 **3.2 Regional differences**

285 Although Figure 1 indicates that the range in k can explain most of the variability in total soil
286 carbon content at equilibrium and hence through transient simulations, Q_{10} is likely to
287 influence the local response of f_T . Figure 5 shows the relative value of f_T for different
288 temperatures and values of Q_{10} . Since the chosen $T_{ref}=15^\circ\text{C}$, all Q_{10} values lead f_T to be equal
289 at this particular temperature. However, the more difference there is between the actual
290 temperature and T_{ref} , the more sensitive f_T becomes to values of Q_{10} . As our simulations are
291 spatially-explicit, this may introduce non-negligible regional differences in C pools at
292 equilibrium and their response to transient changes in T_s and NPP.

293 To investigate this more in detail, we present the zonal averages of soil C density for different
294 values of Q_{10} with k set to 180 months (Figure 6). We choose this particular residence time as
295 example because all corresponding simulations are within the CI₉₅ of the HWSD for 2005
296 regardless the value of Q_{10} . Figure 6a shows that Q_{10} values do introduce non-negligible
297 differences in local equilibrated soil C density. Steady-state pools at low latitudes (30°S to
298 30°N) are larger with low values of Q_{10} (blue in Figure 6). Conversely, high latitude pools are
299 larger with high values of Q_{10} (red in Figure 6). Overall, the range in the value of zonally
300 averaged soil C density at equilibrium is up to three-fold depending on the chosen value of
301 Q_{10} . This is particularly obvious in regions with high NPP including low-latitude tropical
302 rainforests or northern taigas. As was the case with total C_s , the zonal distribution soil C

303 density and the relative position of simulations with different Q_{10} do not vary much between
304 1850 and 2005 (Figure 6b) although there is a slight shift towards uniformly higher densities
305 as all model versions are net global carbon sinks (Figure 2a and 3). The pattern of zonal soil
306 carbon remains essentially the same at the end of RCP 8.5 projections. However, models with
307 lower values of Q_{10} now have more carbon than those with high values of Q_{10} over a broader
308 zone (40°S – 50°N).

309 Figure 7 shows the zonal change in soil C density for the same simulations as in Figure 6.
310 Figure 7a indicates that all simulations simulate a net sink almost everywhere during
311 historical simulations, except at latitudes $> 70^\circ\text{N}$. However, the strength of this sink is
312 strongly dependent upon the value of Q_{10} , especially in low latitudes. There is an
313 approximately two-fold difference between the high accumulation of low Q_{10} models, and the
314 low accumulation of high Q_{10} models. Differences between Q_{10} values are negligible at
315 higher latitudes. Figure 7b shows the same information for RCP 8.5 projections. Simulations
316 with lower values of Q_{10} almost always accumulate more C (except between 0° and 10°N).
317 While all model versions with $k = 180$ months lose carbon at low latitudes ($20^\circ\text{S} - 20^\circ\text{N}$),
318 and gain carbon at high latitudes in the northern hemisphere ($> 50^\circ\text{N}$), the value of Q_{10} , and
319 hence the environmental scalar f_T , decides of the sign of the local soil C balance in the 21st
320 century at mid-latitudes. Within the mid-latitudes, high values of Q_{10} are more likely to
321 simulate a net loss of soil carbon. We can therefore narrow down the dependence of the
322 global ΔC_s on Q_{10} to its affect at mid-latitudes.

323

324 **4 Discussion**

325 **4.1 Effect of k and Q_{10} on soil carbon**

326 In our simulations, the range in total soil carbon at equilibrium (~592 to 2745 Pg C) depends
327 on which value of Q_{10} and especially k is used (Figure 1a). This range captures the ~561 to
328 2938 Pg C range in soil carbon in CMIP-5 in 1860 (see Supplementary Figure S1). We note
329 of course that CMIP5 models not only vary in their soil C component, but simulate different
330 NPP and T_s and also integrate a range of soil moisture limitations (Todd-Brown et al., 2013).
331 The range achieved here at the end of the historical simulations (~709 to 2943 Pg C) is, for
332 example, larger than the 1090 to 2646 Pg C range in 2000 from 7 DGVMs in the ISI-MIP
333 project (Nishina et al., 2014) which were driven by a harmonised weather dataset.

334 We can attribute this range to the first-order representation of decomposition and its response
335 to the initialisation procedure used in most CMIP-5 simulations. By spinning-up the model,
336 the goal is to stabilise pools so that total NPP is exactly compensated by total R_h over the
337 selected period of time (here 10 years). In Equation (2), a longer residence time k results in a
338 lower decay rate (i.e. R_h per unit of C_s). Therefore, model versions that have a slower
339 turnover will require more substrate to simulate the same R_h needed to compensate NPP . As
340 the baseline residence time k is applied globally, it drives the global pool size (Figure 1)
341 much more than changing Q_{10} affects f_T . However, as seen in Figure 6, when considered
342 regionally, Q_{10} plays a non-negligible role for the local response of decomposition and the
343 definition of equilibrium soil C density. High values of Q_{10} lead f_T to trigger strong decay
344 rates in warm regions (Figure 5) that require less substrate (see low latitudes in Figure 6a) to
345 compensate the same NPP . Conversely, high Q_{10} lead to low values of f_T in cold regions.
346 Therefore, more substrate is required to bring the pool to equilibrium as seen in high latitudes
347 in Figure 6a. Low values of Q_{10} show an opposite regional behaviour. Regional differences
348 compensate each other and therefore f_T with different Q_{10} values can only explain a small
349 fraction of the range in equilibrated total soil carbon. Of course, if another T_{ref} was used, the
350 relative differences between f_T with different Q_{10} would be altered and the influence of Q_{10}
351 and its effect on f_T on total and local C_s would vary. Furthermore, the difference between f_T
352 with different Q_{10} grows with the absolute value of the difference $T_s - T_{ref}$. Therefore, using a
353 value of T_{ref} that is outside the range of actual temperatures would lead f_T with different Q_{10} to
354 keep the same relative position globally. It would introduce larger relative differences
355 between these functions.

356 Comparing Figures 1a, 1b and 1c suggests that the range in total C_s at equilibrium is a good
357 predictor of the current and future range in total soil carbon. Despite differences in the
358 magnitude of the change in C_s through time (Friedlingstein et al., 2014), equilibrium
359 conditions achieved under pre-industrial conditions largely define current and future pool
360 sizes. Examining Figure 6 confirms that this global effect can also be seen regionally,
361 especially in low (20°S to 20°N) and high ($>50^\circ\text{N}$) latitudes, where carbon pools are largest.
362 This is of concern as substrate availability also influences R_h and hence its response to
363 changes.

364 Changes in C_s through time are nevertheless non-negligible, and it is important to quantify
365 the response of the system to perturbations. Our results show increasing atmospheric CO_2

366 concentrations enhances NPP more than the simultaneous warming enhances R_h during
367 historical simulations. This historical net carbon sink that is driven by the response of
368 vegetation to increasing atmospheric CO_2 (and hence SOC_{in}) is in accordance with previous
369 studies (Friedlingstein et al., 2006; Sarmiento et al., 2010; Zhang et al., 2011; Wania et al.,
370 2012; Anav et al., 2013; Exbrayat et al., 2013b). Therefore, all model versions with longer
371 residence time accumulate more C_s over the same time period as a result of a slower turnover
372 of carbon in soils, and this mirrors the state of the equilibrium stores. However, despite the
373 dominance of the increased NPP on ΔC_s , the historical warming signal is influential.
374 Specifically, those model versions more sensitive to changes in temperature (i.e. with high
375 values of Q_{10}) accumulate less soil carbon during the 20th century even though they initially
376 equilibrated with larger global pools. This is also true of local soil C density where high Q_{10}
377 values are less accumulating regardless of the initial soil C density. We however note that the
378 value T_{ref} used in our experiments is well within the range of actual temperatures. Therefore,
379 the historical warming does not induce large changes in the values of f_T with different Q_{10} .

380 Projections under the strong-forcing RCP 8.5 scenario also see an increase in the influence of
381 the value of Q_{10} on ΔC_s . Figure 2b clearly shows that the capacity of soils to become carbon
382 sources or remain sinks depends almost entirely on the Q_{10} parameter, and both states can be
383 achieved for any value of k used while remaining within range of previous studies
384 (Friedlingstein et al., 2014; Nishina et al., 2014). Figure 7b indicates that this is clearly a
385 result of differences in the local response of model versions in the mid-latitudes as a function
386 of Q_{10} . Such regional discrepancies leading to a change in the sign of global ΔC_s models have
387 also been highlighted through a recent inter-comparison project that used a harmonised
388 weather dataset to drive 7 biome models (Nishina et al., 2014). However, contrary to this
389 previous study, none of our model versions accumulates soil carbon in the inter-tropical
390 region during the 21st century. This is probably due to the fact that we use the same boundary
391 conditions of NPP and T_s for all our model versions, while models used by Nishina et al.
392 (2013) used a prescribed weather dataset but were left free to simulate their own NPP .

393 Overall, the globally applied model parameter k drives the steady-state response of our
394 reduced complexity system. However, the more conditions are changing (i.e. steady-state to
395 historical to RCP 8.5 projections), the more the dynamic transition of the system towards a
396 new equilibrium depends on the environmental scalar f_T and the specific value of Q_{10} .
397 Although the same formulation of f_T is applied globally, differences in its response to local T_s

398 sum up to determine the sign of total soil carbon balance. We also note that model versions
399 that equilibrate as a result of longer baseline residence time k have a tendency to produce a
400 larger absolute response of total soil carbon balance. Therefore, the size of pools to which the
401 change is applied seems to dominate the response even when higher values of k imply a
402 smaller relative change in the decay rate $k^{-1} \times f_T \times f_W$ used in equation 2. This control of
403 initial conditions obtained by spin-up on the response of the system is a critical aspect that
404 needs to be better resolved, especially since recent inter-comparison experiments all exhibit
405 huge discrepancies in equilibrium conditions of participating models (Anav et al., 2013;
406 Todd-Brown et al., 2013; Nishina et al., 2014).

407

408 **4.2 Discriminating between model versions**

409 Since k clearly influences the total soil carbon content at equilibrium in 1850, it is a good
410 predictor of the current total soil carbon content. Therefore, k is the key parameter that
411 decides how much carbon is active in the modelled system, and whether model versions fall
412 within the CI₉₅ of the HWSD. Here, all simulations with baseline residence time between 150
413 and 250 months fulfil this requirement regardless of which Q_{10} is used in f_T .

414 If we isolate these simulations, the range in total soil carbon change shrinks by 42% and 45%
415 for the historical simulations and RCP 8.5 projections, respectively. However, while this
416 selection dismisses outliers it does not increase confidence in the sign of the soil carbon
417 change. This is because regional differences lead to similar values in total soil carbon for
418 different values of Q_{10} . These regional differences translate into heterogeneous responses
419 under RCP 8.5 forcing, especially in mid-latitudes. They are sufficient to induce a change of
420 sign in the global soil carbon balance.

421

422 **5 Conclusion**

423 We have used a reduced complexity model, broadly representative of current state-of-the-art
424 models of soil organic C decomposition used in CMIP5 and ISI-MIP experiments, to explore
425 the response of microbial decomposition to climate change on soil C dynamics at regional
426 and global scale. We have shown that key parameters in the first-order representation of
427 decomposition interact in markedly different ways depending on the nature of forcing and

428 antecedent conditions. First, the time and space-invariant baseline residence time decides of
429 the total soil carbon content at equilibrium after spin-up, typically the process used by CMIP5
430 models to initialise C pools. Next, the more boundary conditions imposed on the system
431 move away from the equilibrium forcing, the more the environmental scalar describing the
432 sensitivity of the system gains in importance. However, it is the size of the pool to which the
433 change is applied that mostly controls the magnitude of the response.

434 Applying a constraint on total soil carbon that discriminates between acceptable simulations -
435 of total soil carbon leads to a drastic reduction of the range of simulated change. Meanwhile,
436 most of the remaining uncertainty in 21st century projections of total soil carbon can be
437 attributed to zonal differences in the response to change, especially at mid-latitudes. These do
438 not allow us to confidently project soil as either a global source or sink of carbon for the 21st
439 century. However, it is clear that under RCP 8.5 tropical soils are not suited for long-term
440 carbon storage while some more potential exists in high latitudes.

441 Finally, we suggest that future estimates of terrestrial, and especially soil, carbon responses to
442 climate change should be more constrained by available datasets of carbon stocks. This is
443 critical as model structures describe fluxes as a fraction of the substrate pool size. So far, the
444 process of spin-up has too many degrees of freedom that lead to model-specific amounts of
445 active soil carbon.

446

447 **Acknowledgements**

448 This work was supported by the Australian Research Council ARC grant DP110102618 and
449 the ARC Centre of Excellence for Climate System Science grant CE110001028. CSIRO
450 Mk3L model runs were made possible by the NCI National Facility at the Australian National
451 University via the provision of computing resources to the ARC Centre of Excellence for
452 Climate System Science. We thank Dr. K. E. O. Todd-Brown for guidance in processing the
453 HWSD dataset.

454

455 **References**

456 Ahlström, A., Smith, B., Lindström, J., Rummukainen, M., and Uvo, C. B.: GCM
457 characteristics explain the majority of uncertainty in projected 21st century terrestrial

458 ecosystem carbon balance, *Biogeosciences*, 10, 1517-1528, doi:10.5194/bg-10-1517-2013,
459 2013.

460 Allison, S. D., Wallenstein, M. D. and Bradford, M. A.: Soil-carbon response to warming
461 dependent on microbial physiology, *Nat. Geosci.*, 3(5), 336–340, doi:10.1038/ngeo846, 2010.

462 Anav, A., Friedlingstein, P., Kidston, M., Bopp, L., Ciais, P., Cox, P., Jones, C., Jung, M.,
463 Myneni, R., and Zhu, Z.: Evaluating the land and ocean components of the global carbon
464 cycle in the CMIP5 Earth systems models, *J. Clim.*, 26, 6801–6843, doi:10.1175/JCLI-D-12-
465 00417.1, 2013.

466 Bauer, J., Weihermüller, L., Huisman, J., Herbst, M., Graf, A., Séquaris, J. and Vereecken,
467 H.: Inverse determination of heterotrophic soil respiration response to temperature and water
468 content under field conditions, *Biogeochemistry*, 108(1), 119–134, doi:10.1007/s10533-011-
469 9583-1, 2012.

470 Davidson, E. A. and Janssens, I. A.: Temperature sensitivity of soil carbon decomposition
471 and feedbacks to climate change, *Nature*, 440(7081), 165–173, doi:10.1038/nature04514,
472 2006.

473 Exbrayat, J.-F., Pitman, A. J., Abramowitz, G. and Wang, Y.-P.: Sensitivity of net ecosystem
474 exchange and heterotrophic respiration to parameterization uncertainty, *J. Geophys. Res.*
475 *Atmospheres*, 118(4), 1640–1651, doi:10.1029/2012JD018122, 2013a.

476 Exbrayat, J.-F., Pitman, A. J., Zhang, Q., Abramowitz, G., and Wang, Y.-P.: Examining soil
477 carbon uncertainty in a global model: response of microbial decomposition to temperature,
478 moisture and nutrient limitation, *Biogeosciences*, 10, 7095-7108, doi:10.5194/bg-10-7095-
479 2013, 2013b.

480 Exbrayat, J.-F., Pitman, A. J., and Abramowitz, G.: Response of microbial decomposition to
481 spin-up explains CMIP5 soil carbon range until 2100, *Geosci. Model Dev. Discuss.*, 7, 3481-
482 3504, doi:10.5194/gmdd-7-3481-2014, 2014.

483 Falloon, P. D., Jones, C. D., Ades, M. and Paul, K.: Direct soil moisture controls of future
484 global soil carbon changes: An important source of uncertainty, *Glob. Biogeochem. Cycles*,
485 25, GB3010, doi: 10.1029/2010GB003938, 2011.

486 FAO/IIASA/ISRIC/ISSCAS/JRC: Harmonized World Soil Database (version 1.21), FAO,
487 Rome, Italy and IIASA, Laxenburg, Austria, 2012.

488 Friedlingstein, P., Cox, P., Betts, R., Bopp, L., von Bloh, W., Brovkin, V., Cadule, P., Doney,
489 S., Eby, M., Fung, I., Bala, G., John, J., Jones, C., Joos, F., Kato, T., Kawamiya, M., Knorr,
490 W., Lindsay, K., Matthews, H. D., Raddatz, T., Rayner, P., Reick, C., Roeckner, E.,
491 Schnitzler, K.-G., Schnur, R., Strassmann, K., Weaver, A. J., Yoshikawa, C. and Zeng, N.:
492 Climate–Carbon Cycle Feedback Analysis: Results from the C⁴MIP Model Intercomparison,
493 *J. Clim.*, 19, 3337–3353, doi:10.1175/JCLI3800.1, 2006.

494 Friedlingstein, P., Meinhausen, M., Arora, V. K., Jones, C. D., Anav, A., Liddicoat, S. K.,
495 and Knutti, R.: Uncertainties in CMIP5 climate projections due to carbon cycle feedbacks, *J.*
496 *Clim.*, 27, 511–526, doi:10.1175/JCLI-D-12-00579.1, 2014.

497 Friend, A. D., et al: Carbon residence time dominates uncertainty in terrestrial vegetation
498 responses to future climate and atmospheric CO₂, *Proc. Natl. Acad. Sci.*, in press, 2013.

499 Kirschbaum, M. U. F.: Soil respiration under prolonged soil warming: are rate reductions
500 caused by acclimation or substrate loss?, *Glob. Change Biol.*, 10(11), 1870–1877,
501 doi:10.1111/j.1365-2486.2004.00852.x, 2004.

502 Knorr, W., Prentice, I. C., House, J. I. and Holland, E. A.: Long-term sensitivity of soil
503 carbon turnover to warming, *Nature*, 433(7023), 298–301, doi:10.1038/nature03226, 2005.

504 Koven, C. D., Ringeval, B., Friedlingstein, P., Ciais, P., Cadule, P., Khvorostyanov, D.,
505 Krinner, G. and Tarnocai, C.: Permafrost carbon-climate feedbacks accelerate global
506 warming, *Proc. Natl. Acad. Sci.*, 108(36), 14769–14774, doi:10.1073/pnas.1103910108,
507 2011.

508 Lloyd, J. and Taylor, J. A.: On the Temperature Dependence of Soil Respiration, *Funct.*
509 *Ecol.*, 8(3), 315–323, doi:10.2307/2389824, 1994.

510 Luo, Y., Wan, S., Hui, D. and Wallace, L. L.: Acclimatization of soil respiration to warming
511 in a tall grass prairie, *Nature*, 413(6856), 622–625, doi:10.1038/35098065, 2001.

512 Mahecha, M. D., Reichstein, M., Carvalhais, N., Lasslop, G., Lange, H., Seneviratne, S. I.,
513 Vargas, R., Ammann, C., Arain, M. A., Cescatti, A., Janssens, I. A., Migliavacca, M.,
514 Montagnani, L. and Richardson, A. D.: Global Convergence in the Temperature Sensitivity
515 of Respiration at Ecosystem Level, *Science*, 329(5993), 838–840,
516 doi:10.1126/science.1189587, 2010.

517 Nishina, K., Ito, A., Beerling, D. J., Cadule, P., Ciais, P., Clark, D. B., Falloon, P., Friend, A.
518 D., Kahana, R., Kato, E., Keribin, R., Lucht, W., Lomas, M., Rademacher, T. T., Pavlick, R.,
519 Schaphoff, S., Vuichard, N., Warszawski, L., and Yokohata, T.: Quantifying uncertainties in
520 soil carbon responses to changes in global mean temperature and precipitation, *Earth Syst.*
521 *Dynam.*, 5, 197-209, doi:10.5194/esd-5-197-2014, 2014.

522 Phipps, S. J., L. D. Rotstayn, H. B. Gordon, J. L. Roberts, A. C. Hirst and W. F. Budd: The
523 CSIRO Mk3L climate system model version 1.0 - Part 1: Description and evaluation,
524 *Geoscientific Model Development*, 4, 483-509, doi:10.5194/gmd-4-483-2011, 2011.

525 Sarmiento, J. L., Gloor, M., Gruber, N., Beaulieu, C., Jacobson, A. R., Mikaloff Fletcher, S.
526 E., Pacala, S. and Rodgers, K.: Trends and regional distributions of land and ocean carbon
527 sinks, *Biogeosciences*, 7(8), 2351–2367, doi:10.5194/bg-7-2351-2010, 2010.

528 Tarnocai, C., Canadell, J. G., Schuur, E. a. G., Kuhry, P., Mazhitova, G. and Zimov, S.: Soil
529 organic carbon pools in the northern circumpolar permafrost region, *Glob. Biogeochem.*
530 *Cycles*, 23(2), GB2023, doi:10.1029/2008GB003327, 2009.

531 Taylor, K. E., Stouffer, R. J. and Meehl, G. A.: An Overview of CMIP5 and the Experiment
532 Design, *Bull. Am. Meteorol. Soc.*, 93(4), 485–498, doi:10.1175/BAMS-D-11-00094.1, 2012.

533 Todd-Brown, K. E. O., Randerson, J. T., Post, W. M., Hoffman, F. M., Tarnocai, C., Schuur,
534 E. A. G., and Allison, S. D.: Causes of variation in soil carbon simulations from CMIP5 Earth
535 system models and comparison with observations, *Biogeosciences*, 10, 1717-1736,
536 doi:10.5194/bg-10-1717-2013, 2013.

537 Todd-Brown, K. E. O., Hopkins, F. M., Kivlin, S. N., Talbot, J. M. and Allison, S. D.: A
538 framework for representing microbial decomposition in coupled climate models,
539 *Biogeochemistry*, 109(1), 19–33, doi:10.1007/s10533-011-9635-6, 2012.

540 Wang, Y. P., Kowalczyk, E., Leuning, R., Abramowitz, G., Raupach, M. R., Pak, B., Gorsel,
541 E. van and Luhar, A.: Diagnosing errors in a land surface model (CABLE) in the time and
542 frequency domains, *J. Geophys. Res.*, 116, G01034, doi:10.1029/2010JG001385, 2011.

543 Wang, Y. P., Law, R. M. and Pak, B.: A global model of carbon, nitrogen and phosphorus
544 cycles for the terrestrial biosphere, *Biogeosciences*, 7(7), 2261–2282, doi:10.5194/bg-7-2261-
545 2010, 2010.

546 Wania, R., Meissner, K. J., Eby, M., Arora, V. K., Ross, I., and Weaver, A. J.: Carbon-
547 nitrogen feedbacks in the UVic ESCM, *Geosci. Model Dev.*, 5, 1137-1160, doi:10.5194/gmd-
548 5-1137-2012, 2012.

549 Wieder, W. R., Bonan, G. B and Allison, S. D., Global soil carbon projections are improved
550 by modelling microbial processes, *Nature Clim. Change* 3, 909–912,
551 doi:10.1038/nclimate1951, 2013.

552 Xenakis, G. and Williams, M., Comparing microbial and chemical approaches for modelling
553 soil organic carbon decomposition using the DecoChem v1.0 and DecoBio v1.0 models,
554 *Geosci. Model. Dev. Discuss.*, 7, 33-72, doi:10.5194/gmdd-7-33-2014, 2014.

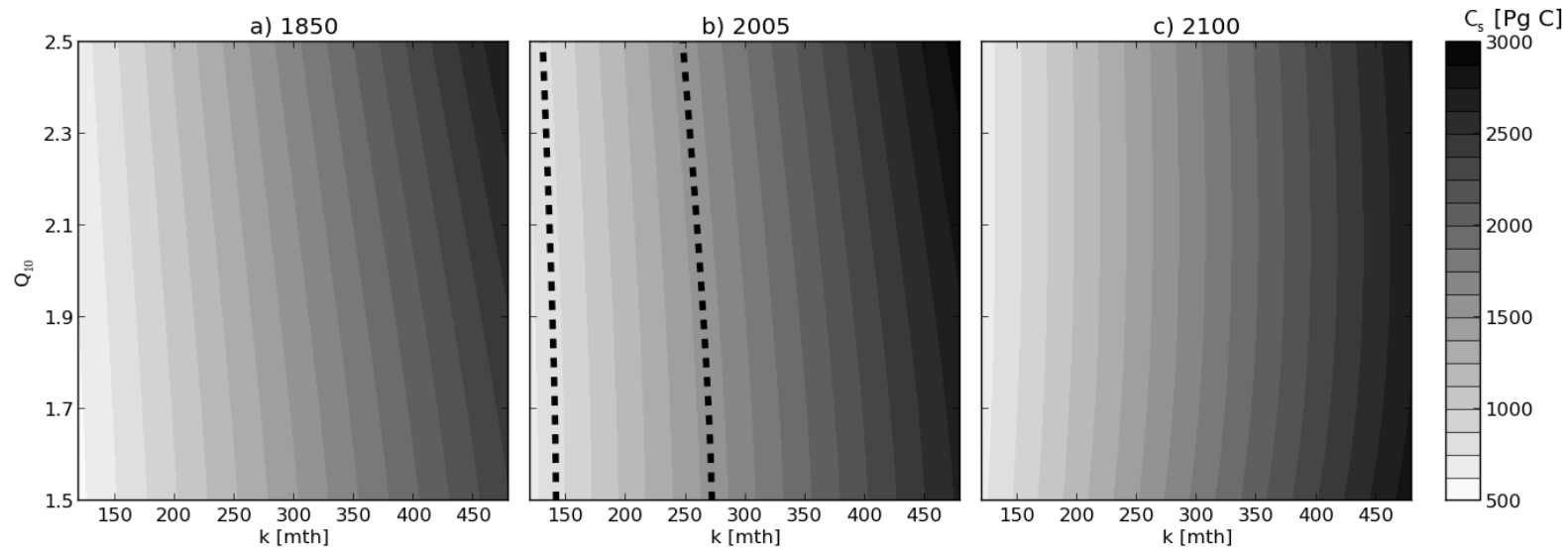
555 Xia, J. Y., Luo, Y. Q., Wang, Y.-P., Weng, E. S., and Hararuk, O.: A semi-analytical solution
556 to accelerate spin-up of a coupled carbon and nitrogen land model to steady state, *Geosci.*
557 *Model Dev.*, 5, 1259-1271, doi:10.5194/gmd-5-1259-2012, 2012.

558 Xia, J., Luo, Y., Wang, Y.-P. and Hararuk, O.: Traceable components of terrestrial carbon
559 storage capacity in biogeochemical models. *Glob. Change Biol.*, 19, 2104–2116. doi:
560 10.1111/gcb.12172, 2013.

561 Zhang, Q., Wang, Y. P., Pitman, A. J. and Dai, Y. J.: Limitations of nitrogen and
562 phosphorous on the terrestrial carbon uptake in the 20th century, *Geophys. Res. Lett.*, 38,
563 L22701, doi:10.1029/2011GL049244, 2011.

564

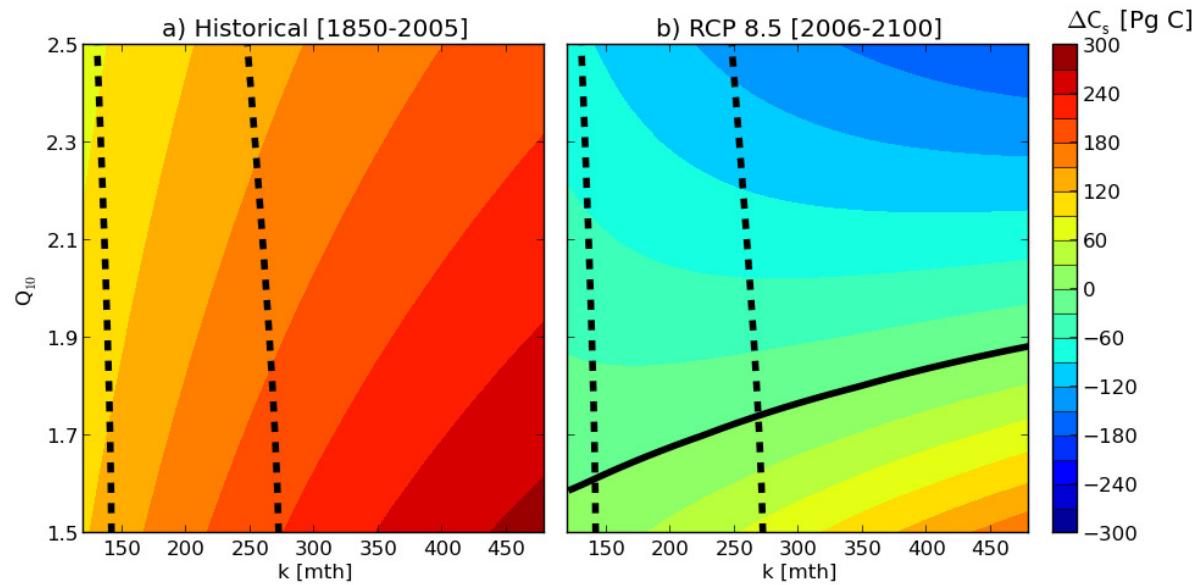
565



566

567 **Figure 1.** Snapshots of total soil carbon in the reduced complexity model as a function of parameter values. Dashed contours in panel b indicate
 568 the CI₉₅ of the HWSD in 2005 (830 – 1550 Pg C).

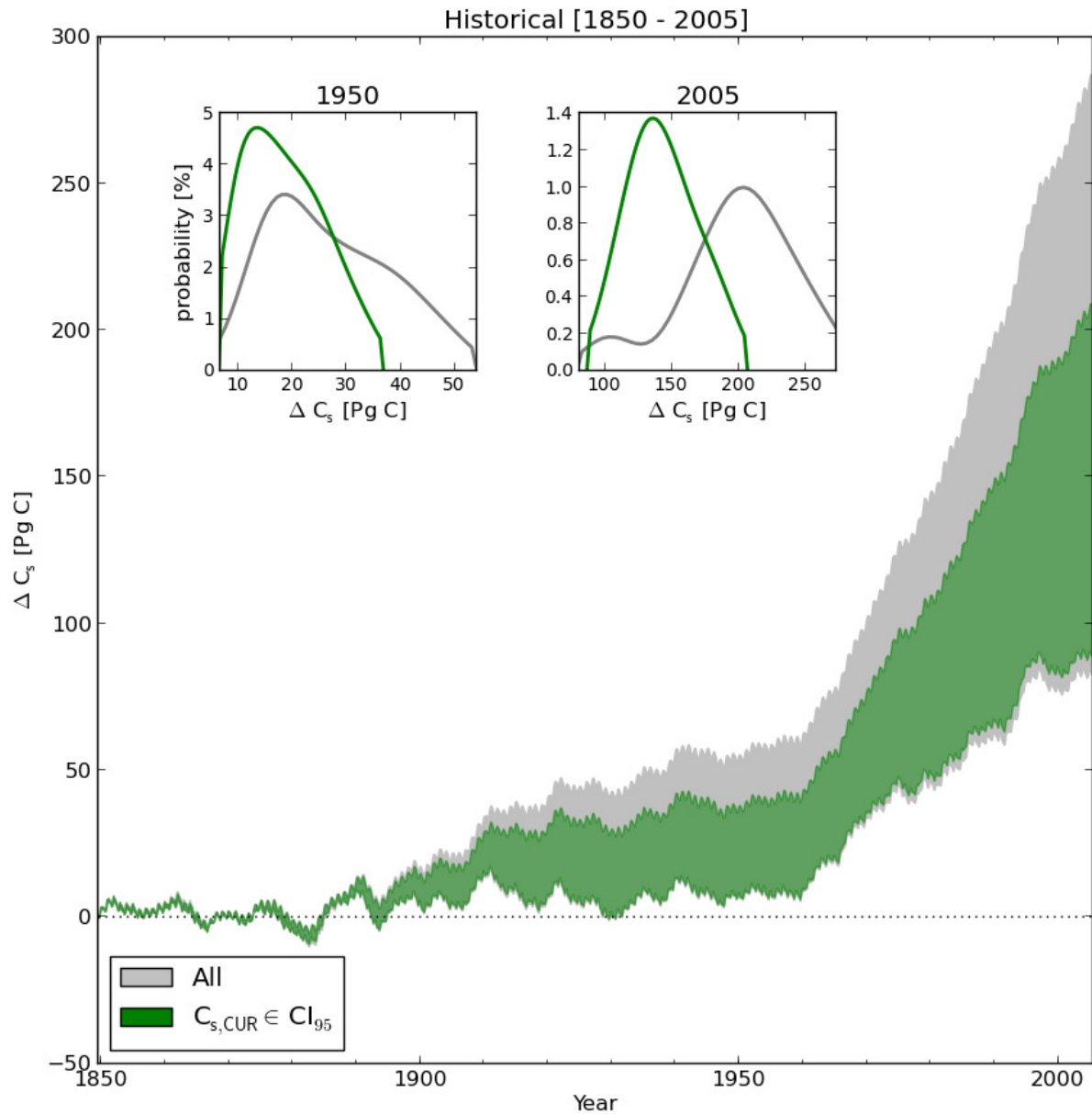
569



570

571 **Figure 2.** Change in total soil carbon in the reduced complexity model as a function of parameter values for each period as indicated. Dashed
 572 contours in panel b indicate model versions that produced soil stocks within the CI_{95} of the HWSD in 2005 (830 – 1550 Pg C). The thick black
 573 line represents no change.

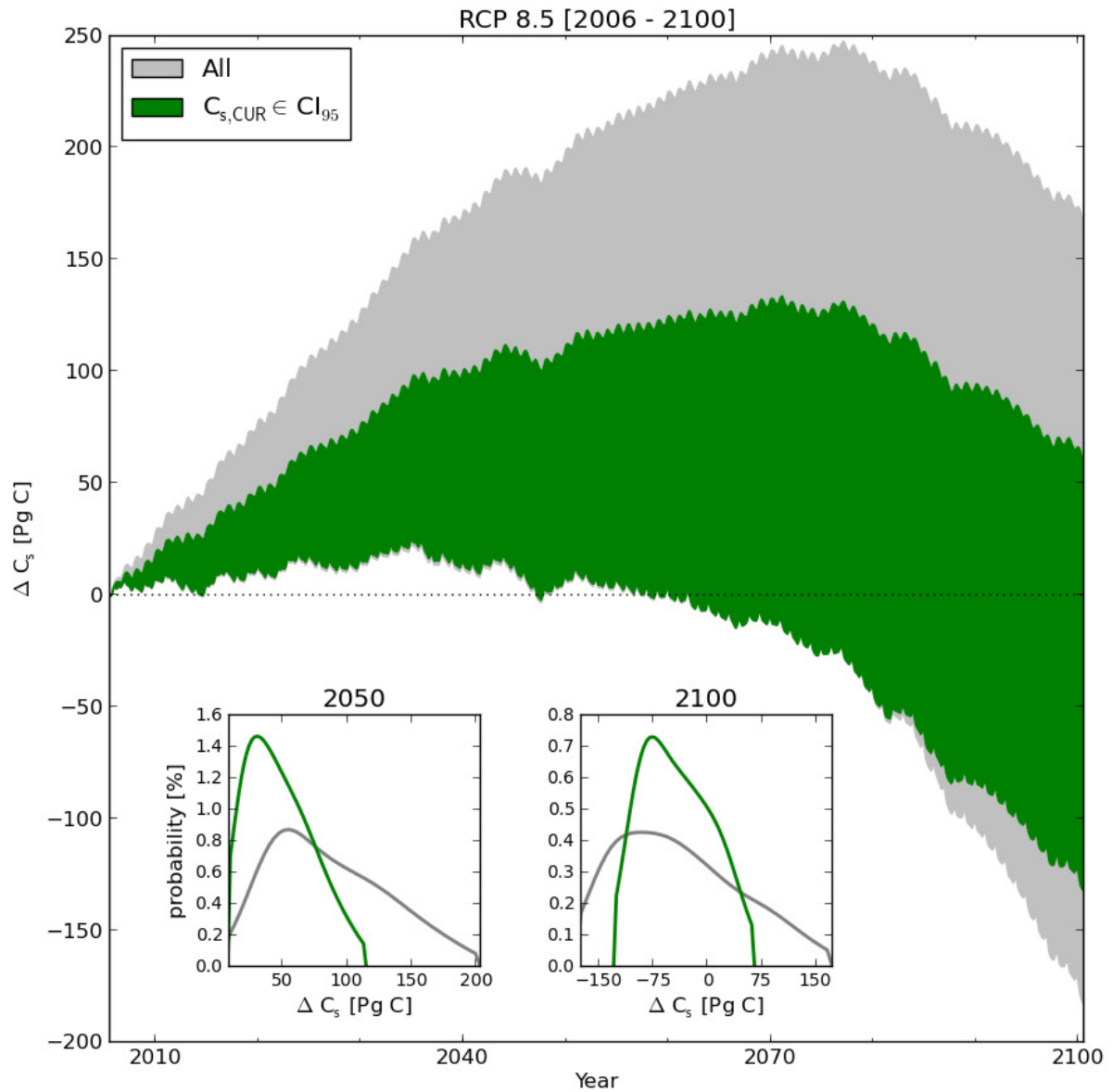
574



575

576 **Figure 3.** Change in total soil carbon through time for historical simulations. Insets represent
 577 the probability density function of the change since 1850 for the period indicated. Grey is for
 578 all simulations while green is used to distinguish simulations for which total soil carbon is
 579 within the CI_{95} of the HWSO in 2005.

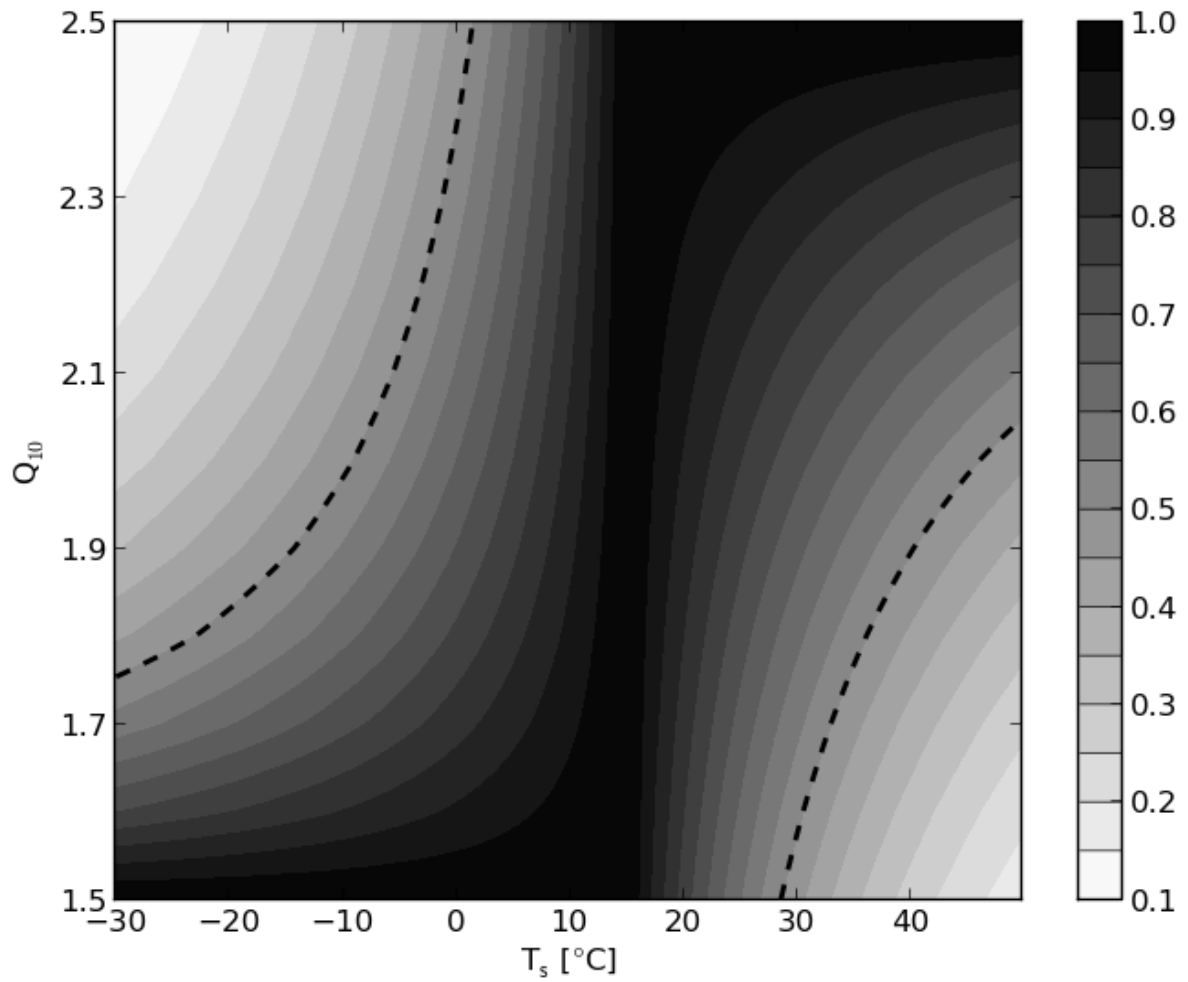
580



581

582 **Figure 4.** Change in total soil carbon through time for RCP 8.5 projections. Insets represent
 583 the probability density function of the change since 2005 for the indicated year. Grey is for
 584 all simulations while green is used to distinguish simulations for which total soil carbon is
 585 within the CI_{95} of the HWSD in 2005.

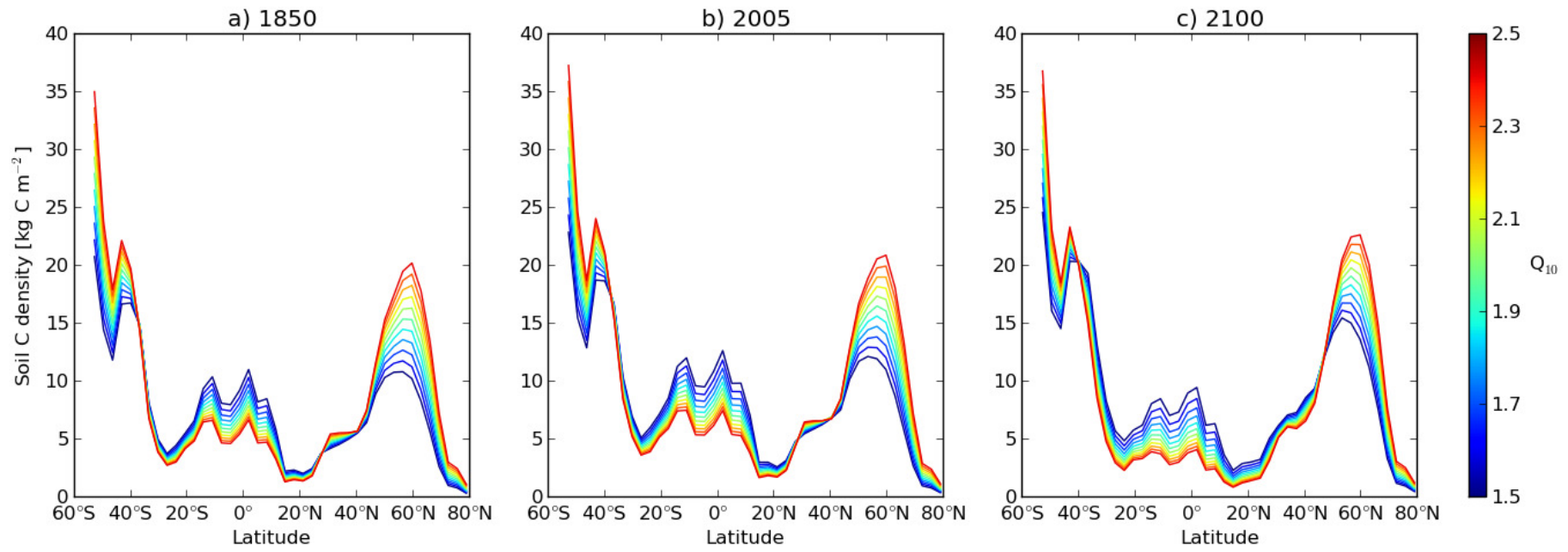
586



587

588 **Figure 5.** Values of f_T as a function of T_s and Q_{10} . For each temperature, the value is
 589 expressed as the proportion of the maximum value achieved for any value of Q_{10} . Areas
 590 outside of the dashed lines represent where f_T is less than 50% of the maximum for the same
 591 temperature.

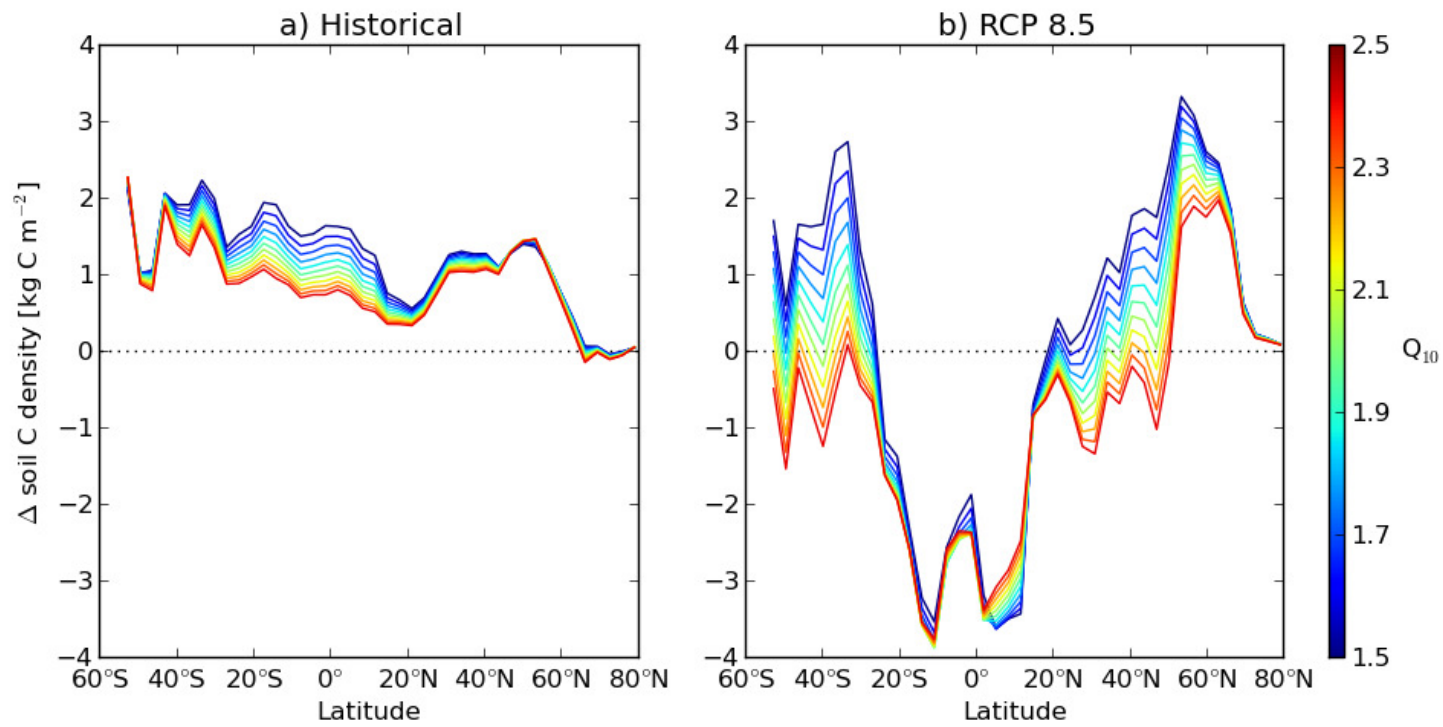
592



593

594 **Figure 6.** Zonal average soil carbon density in the reduced complexity model with $k=180$ months and various values of Q_{10} as indicated by the
 595 colour bar.

596



597

598 **Figure 7.** Zonal change in soil C density during historical simulations (a) and RCP8.5 (b)

599

600